Lithium–Air Batteries

Deutsche Ausgabe: DOI: 10.1002/ange.201602142
Internationale Ausgabe: DOI: 10.1002/anie.201602142

Singlet Oxygen Formation during the Charging Process of an Aprotic Lithium–Oxygen Battery

Johannes Wandt, Peter Jakes,* Josef Granwehr, Hubert A. Gasteiger, and Rüdiger-A. Eichel*

Abstract: *Aprotic lithium–oxygen ($Li–O_2$) batteries have attracted considerable attention in recent years owing to their outstanding theoretical energy density. A major challenge is their poor reversibility caused by degradation reactions, which mainly occur during battery charge and are still poorly understood. Herein, we show that singlet oxygen ($^1\Delta_g$) is formed upon Li_2O_2 oxidation at potentials above 3.5 V. Singlet oxygen was detected through a reaction with a spin trap to form a stable radical that was observed by time- and voltage-resolved in operando EPR spectroscopy in a purpose-built spectroelectrochemical cell. According to our estimate, a lower limit of approximately 0.5 % of the evolved oxygen is singlet oxygen. The occurrence of highly reactive singlet oxygen might be the long-overlooked missing link in the understanding of the electrolyte degradation and carbon corrosion reactions that occur during the charging of $Li–O_2$ cells.*

Since its discovery,[1] the aprotic lithium–air or lithium–oxygen ($Li–O_2$) battery has attracted huge interest as a possible "beyond-lithium-ion" technology owing to its outstanding theoretical energy density of 3460 $Wh\,kg^{-1}$.[2] The energy density on a system level—taking into account inactive cell components—has been predicted to lie between 250 and 500 $Wh\,kg^{-1}$, which exceeds a current lithium-ion battery by a factor of about 1.5 to 2.[3] The central problem for the development of a reversible $Li–O_2$ cell chemistry are parasitic side reactions causing the degradation of both the carbon electrode and the electrolyte upon battery cycling, thus leading to cell death within a few cycles.[4,5] In the reversible formation of Li_2O_2 ($2\,Li^+ + O_2 + 2\,e^- \rightarrow Li_2O_2$), an important measure to quantify the contribution of undesired side reactions is the e^-/O_2 ratio, which should ideally equal 2.00. However, several research groups found that, especially during charging, e^-/O_2 ratios significantly deviate from 2.00 for various combinations of solvents, conducting salts, and cathode materials.[6,7] The exact electrochemical or chemical nature of the side reactions during charge remains largely unclear, but some form of "nascent" oxygen produced during charging has been suggested to contribute to the degradation of several cell components.[8] This hypothesis is consistent with the observation that ^{13}C-labeled carbon electrodes show an onset of carbon corrosion at 3.5 V during Li_2O_2 oxidation, even though carbon is generally considered stable to potentials well above 4.0 V in the absence of Li_2O_2,[9] which led to the conclusion that *"the process of carbon decomposition involves Li_2O_2 or its intermediates of oxidation"*.[10]

Singlet oxygen (term symbol $^1\Delta_g$, hereafter $^1O_2$) could potentially be this reactive intermediate.[11] It is a strong oxidizing agent and known to form upon chemical oxidation of Li_2O_2, Na_2O_2, and a series of organic peroxides.[12,13] The thermodynamically reversible potential for $^1O_2$ evolution during the electrooxidation of Li_2O_2 can be estimated to be between 3.45 and 3.55 V, only about 0.5 V higher than its reversible potential to triplet oxygen (term symbol $^3\Sigma_g^-$), $U_0 =$ 2.96 V.[14] This estimate is derived from $U_0 + \Delta G(^3\Sigma_g^- \rightarrow {}^1\Delta_g)/2F$, in which F is the Faraday constant and $\Delta G(^3\Sigma_g^- \rightarrow {}^1\Delta_g)$ is the difference in Gibbs free energy between singlet and triplet oxygen; $\Delta G(^3\Sigma_g^- \rightarrow {}^1\Delta_g)$ can be estimated from $\Delta H(^3\Sigma_g^- \rightarrow {}^1\Delta_g) = 94\ kJ\,mol^{-1}$ and the assumption $0\ kJ\,mol^{-1} < -T\Delta S(^3\Sigma_g^- \rightarrow {}^1\Delta_g) < 20\ kJ\,mol^{-1}$.[15,16] The reversible potential for $^1O_2$ formation fits the observed onset potential for carbon corrosion well; however, the possibility of $^1O_2$ formation during charge in $Li–O_2$ batteries has been largely overlooked. To the best of our knowledge, there have been no experimental investigations and only a few mentions of $^1O_2$ in the context of $Li–O_2$ batteries. A potential of around 3.9 V[6,11,17–19] as the thermodynamic threshold for $^1O_2$ evolution has been stated, neglecting that the energy transfer takes place in a two-electron process and that $^1O_2$ evolution could therefore already occur at lower potentials, as shown above. Consequently, $^1O_2$ evolution was considered a less likely source of side reactions during charge.[6]

We herein present the first experimental investigation of $^1O_2$ formation during the charge of an aprotic $Li–O_2$ battery. The identification of $^1O_2$ is based on its reactivity towards a specific spin trap to form a stable radical that can be detected by in operando electron paramagnetic resonance (EPR) spectroscopy.[20]

Sterically hindered secondary amines have long been used to detect $^1O_2$.[21] Scheme 1 shows the reaction of 2,2,6,6-

[*] J. Wandt, H. A. Gasteiger
Technische Universität München
Chair for Technical Electrochemistry, Department of Chemistry and Catalysis Research Center (Germany)
E-mail: johannes.wandt@tum.de
P. Jakes, J. Granwehr, R.-A. Eichel
Forschungszentrum Jülich, Institut für Energie- und Klimaforschung
Grundlagen der Elektrochemie (IEK-9)
52425 Jülich (Germany)
E-mail: p.jakes@fz-juelich.de
R.-A. Eichel
RWTH Aachen University, Institut für Physikalische Chemie
52074 Aachen (Germany)
J. Granwehr
RWTH Aachen University
Institut für Technische und Makromolekulare Chemie
52074 Aachen (Germany)
Supporting information and the ORCID identification number(s) for the author(s) of this article can be found under http://dx.doi.org/10.1002/anie.201602142.

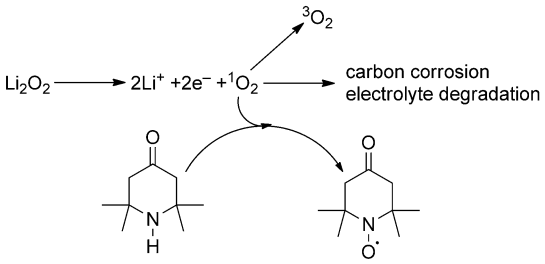

Scheme 1. Chemical reaction underlying the spin-trap approach: The reaction of 4-Oxo-TEMP with singlet oxygen forms the stable 4-Oxo-TEMPO radical, which is detected by in operando EPR spectroscopy. The trapping reaction is in kinetic competition with $^1O_2$ relaxation to triplet oxygen and other chemical reactions.

tetramethyl-4-piperidone (4-Oxo-TEMP) with $^1O_2$ to form 4-Oxo-2,2,6,6-tetramethyl-1-piperidinyloxy (4-Oxo-TEMPO), which is a stable radical that can be identified by its characteristic EPR spectrum. 4-Oxo-TEMP is a very selective trapping agent for $^1O_2$,[22,23] especially as it does not react with superoxide radicals.[24] It is added to the electrolyte in a rather high concentration of 0.1 M, as the trapping reaction is in kinetic competition with $^1O_2$ relaxation to triplet oxygen, which is fast in liquid media ($\tau_{1/2} \approx 10^{-6}$–$10^{-3}$ s).[25,26] To investigate whether the spin trap reacted with Li_2O_2, discharged electrodes containing Li_2O_2 were stored either in standard electrolyte or 4-Oxo-TEMP-containing electrolyte. After storage, the same peroxide content was found in the electrode,[27] irrespective of the absence or presence of 4-Oxo-TEMP, thus ruling out a redox reaction. Furthermore, no dissolved peroxide species were found in the electrolyte, thus ruling out an acid–base reaction between Li_2O_2 and 4-Oxo-TEMP (see the Supporting Information). To verify that the presence of 4-Oxo-TEMP did not alter the electrochemical charging process, we determined the oxygen-evolution rates by on-line electrochemical mass spectrometry (OEMS; see the Supporting Information). In the presence of 4-Oxo-TEMP, Li_2O_2 oxidation proceeded normally up to a potential of about 3.9 V, when severe side reactions set in.

In operando EPR experiments were conducted with a custom spectroelectrochemical cell (Figure 1), which could be cycled directly within the cavity of the EPR spectrometer.[20] The housing was adapted to facilitate purging of the cell with gas, and a reference electrode was incorporated for potential-controlled experiments. The in operando EPR cell consisted of a Vulcan electrode containing Li_2O_2 coated on a Celgard separator, a glassfiber separator, chemically delithiated LFP as a counter electrode, and 0.5 M bis(trifluoromethane)sulfonimide lithium salt (LiTFSI) and 0.1 M 4-Oxo-TEMP in diglyme as the electrolyte (see the Supporting Information).

Figure 2 shows a typical charging curve recorded in the EPR cell. Only the charging step is done in the EPR cell; the prior discharge is carried out in a standard cell with the standard electrolyte (inset in Figure 2a), from which the Li_2O_2-containing Vulcan electrode is harvested. Figure 2b shows EPR spectra recorded in the in operando EPR cell during charge at positions indicated by the blue circles in

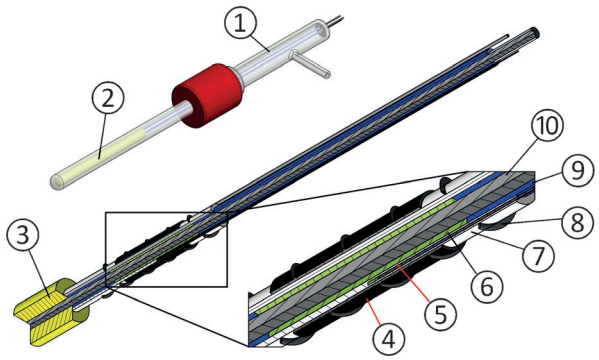

Figure 1. In operando EPR cell design. Top left: Cell housing with ① lid containing a connection for gas purging and three feed-through wires for contacting of working, counter, and reference electrodes; ② EPR tube containing the electrochemical cell. Center: Tubular electrochemical cell with ③ poly(tetrafluoroethylene) (PTFE) spacer. Bottom right: Cut through electrochemical cell, ④ Vulcan working electrode coated on Celgard separator, ⑤ reference electrode, ⑥ LFP counter electrode coated on Al wire (⑩), ⑦ glass-fiber separator, ⑧ Al wire (0.1 mm diameter) as working-electrode current collector, ⑨ PTFE tube, ⑩ Al wire (2.0 mm diameter) as counter electrode current collector.

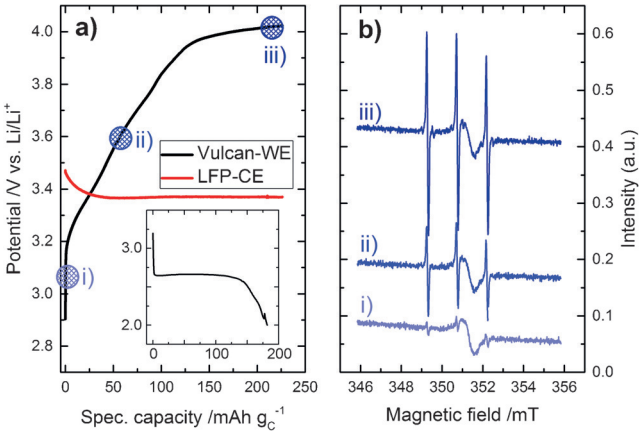

Figure 2. a) Charging curve ($i = 60$ mA g_C^{-1}) of Li_2O_2 in an in operando EPR cell with 0.5 M LiTFSI in diglyme containing 0.1 M 4-Oxo-TEMP as a spin trap under an argon atmosphere; inset: previous discharge ($i = 120$ mA g_C^{-1}) in a standard cell under an oxygen atmosphere. b) In operando EPR spectra (10 spectra averaged), recorded at the different charging potentials as indicated in (a).

Figure 2a. The initial spectrum shows a broad and featureless peak at $g = 2.0029$ from carbon dangling bonds and three narrow lines caused by a small amount of 4-Oxo-TEMPO impurity already present in the electrolyte. The later spectra clearly show the increased characteristic 1:1:1 triplet signal of 4-Oxo-TEMPO, which is the only EPR-active species formed during the entire charge process. The slanted baseline present in all three spectra can be assigned to a very broad EPR signal from the LFP counter electrode.

From the peak-to-peak amplitude of the EPR resonances (Figure 2b), it is possible to extract the relative amount of 4-Oxo-TEMPO (see the Supporting Information). Figure 3

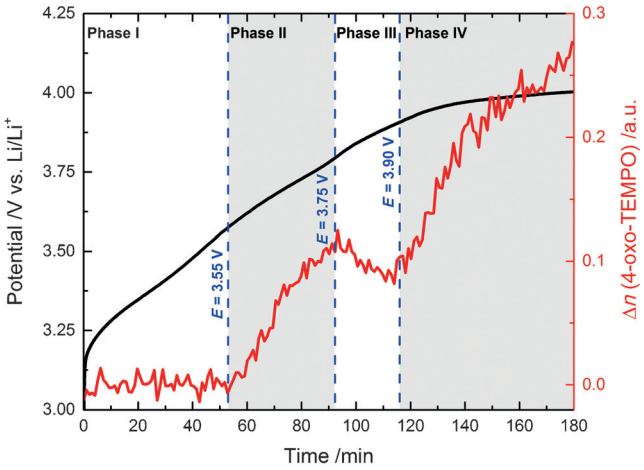

Figure 3. Voltage profile and EPR signal amplitude for 4-Oxo-TEMPO formed during the charging ($i = 60\ mA\ g_C^{-1}$) of Li_2O_2 with 0.5 M LiTFSI in diglyme containing 0.1 M 4-Oxo-TEMP as a spin trap.

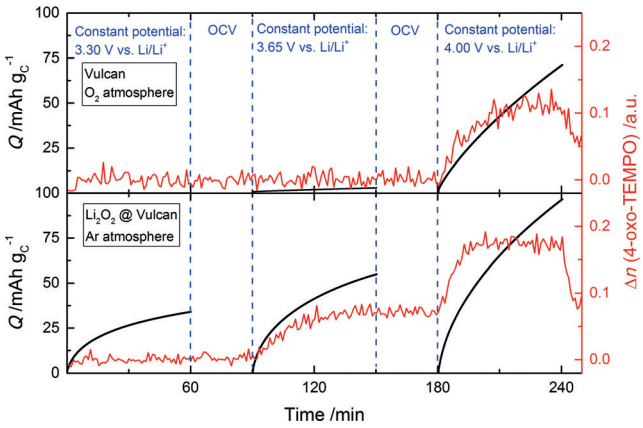

Figure 4. Charging capacity (black lines) and evolution of 4-Oxo-TEMPO EPR signal intensity (red lines) during potential stepping experiments. Top: Fresh Vulcan electrode without Li_2O_2 under oxygen (0.5 bar) and argon (0.5 bar). Bottom: Li_2O_2-containing Vulcan electrode under argon (1 bar). Electrolyte: 0.5 M LiTFSI in diglyme with 4-Oxo-TEMP.

shows the evolution of the 4-Oxo-TEMPO signal and the corresponding cell potential during charge, which can be separated into four distinct phases. During phase I and II, a normal charging process with Li_2O_2 oxidation as the main electrochemical reaction occurs, as indicated by the oxygen-evolution curve determined by OEMS (see Figure S6 in the Supporting Information). The 4-Oxo-TEMPO amount starts to increase once the electrode potential exceeds about 3.55 V, which is close to the thermodynamic threshold for $^1O_2$ formation (3.45–3.55 V), thus suggesting that this increase is caused by the reaction of the spin trap with $^1O_2$ (Scheme 1). During phase III, the 4-Oxo-TEMPO concentration decreases as a result of the $1\,e^-$ oxidation of the nitroxyl radical, a reaction known to occur in this potential range.[28–30] Above approximately 3.9 V during phase IV, another increase in the amount of 4-Oxo-TEMPO is accompanied by the consumption of oxygen, as seen in the OEMS data. The spin trap is electrochemically oxidized, which triggers a reaction with triplet oxygen to form 4-Oxo-TEMPO.[24,31] The presence of these four phases shows that a time- and voltage-resolved in operando EPR experiment is critical for unraveling the different mechanisms for the formation and decomposition of 4-Oxo-TEMPO (Figure 3).

To further provide evidence for the assignment of the electrochemical and chemical reactions to phases I–IV and that the increase in 4-Oxo-TEMPO during phase II is caused by $^1O_2$, we carried out potential-controlled experiments. Three different potentials were applied for 60 min each, with 30 min open-circuit (OCV) periods in between. The first potential of 3.3 V is below the thermodynamic threshold for $^1O_2$ formation, the second potential of 3.65 V is above this threshold but well within the stability window of the spin trap, and the third potential of 4.0 V is in the range in which the spin trap is electrochemically oxidized. The upper panel in Figure 4 shows that in the absence of Li_2O_2, 4-Oxo-TEMPO is only formed at 4.0 V, thus confirming that the increase observed during phase II in Figure 3 must be linked to Li_2O_2 oxidation. The fact that the oxidation of Li_2O_2 at 3.30 V does not yield 4-Oxo-TEMPO (lower panel in Figure 4) rules out the formation of 4-Oxo-TEMPO upon Li_2O_2 oxidation as a result of some unspecified side reaction. If the Li_2O_2 oxidation potential is then increased to 3.65 V, the formation of 4-Oxo-TEMPO sets in instantaneously, and can thus only be assigned to the reaction between $^1O_2$ and the spin trap.

In conclusion, in operando EPR data (Figures 3 and 4), in combination with OEMS data (see Figure S6), unambiguously show that $^1O_2$ is evolved at potentials above about 3.55 V in the charging process of aprotic Li–O_2 batteries. The EPR data were also reproduced in a second in operando EPR cell design with a conventional flat-cell configuration. The same four reaction phases with identical onset potentials were observed in the flat cell (see the Supporting Information).

To estimate the proportion of $^1O_2$, the amount of 4-Oxo-TEMPO formed in the range from 3.55 to 3.75 V (phase II, Figure 3) has been quantified by a calibration procedure with a known amount of 4-Oxo-TEMPO (see the Supporting Information). The total amount of evolved oxygen is estimated by the respective capacity and the e^-/O_2 ratio determined by OEMS. On the basis of the assumption that 100 % of the $^1O_2$ formed during charging is converted into 4-Oxo-TEMPO, a lower limit of approximately 0.5 % $^1O_2$ can be calculated. The real fraction of $^1O_2$ is most likely higher, as a significant part of the evolved $^1O_2$ will be quenched by the solvent or other side reactions before being trapped. However, this simple estimate already shows that $^1O_2$ is formed in substantial quantities. The close proximity of the onset potentials for $^1O_2$ evolution and carbon corrosion reactions at about 3.5 V suggests that $^1O_2$ as a highly reactive oxidizing species might play a central role in irreversible side reactions during the charging of Li–O_2 batteries. In a next step, it will first be necessary to quantify the extent to which $^1O_2$ is involved in parasitic side reactions during charge. Targeted counter measures can then be developed to eliminate $^1O_2$-induced side reactions and improve the reversibility and cycle life of Li–O_2 batteries.

Acknowledgements

We thank Anna Freiberg (TUM), Cyril Marino (Paul-Scherrer-Institut, Switzerland), and Yi-Chun Lu (Chinese University of Hongkong) for contributions to the EPR cell design and Juan Herranz (Paul-Scherrer-Institut, Switzerland) for experimental support. TUM gratefully acknowledges financial support by the Bavarian Ministry of Economic Affairs and Media, Energy and Technology under the auspices of the EEBatt project. Forschungszentrum Jülich gratefully acknowledges financial support by the German Ministry of Education and Research (BMBF) within the framework of the MEET-HiEnD project.

Keywords: carbon corrosion · charging mechanism · EPR spectroscopy · lithium–air batteries · singlet oxygen

How to cite: *Angew. Chem. Int. Ed.* **2016**, *55*, 6892 – 6895
Angew. Chem. **2016**, *128*, 7006 – 7009

[1] K. M. Abraham, Z. Jiang, *J. Electrochem. Soc.* **1996**, *143*, 1 – 5.
[2] J. Christensen, P. Albertus, R. S. Sanchez-Carrera, T. Lohmann, B. Kozinsky, R. Liedtke, J. Ahmed, A. Kojic, *J. Electrochem. Soc.* **2012**, *159*, R1 – R30.
[3] K. G. Gallagher, S. Goebel, T. Greszler, M. Mathias, W. Oelerich, D. Eroglu, V. Srinivasan, *Energy Environ. Sci.* **2014**, *7*, 1555 – 1563.
[4] S. A. Freunberger, Y. Chen, N. E. Drewett, L. J. Hardwick, F. Bardø, P. G. Bruce, *Angew. Chem. Int. Ed.* **2011**, *50*, 8609 – 8613; *Angew. Chem.* **2011**, *123*, 8768 – 8772.
[5] Y.-C. Lu, B. M. Gallant, D. G. Kwabi, J. R. Harding, R. R. Mitchell, M. S. Whittingham, Y. Shao-Horn, *Energy Environ. Sci.* **2013**, *6*, 750 – 786.
[6] B. D. McCloskey, D. S. Bethune, R. M. Shelby, T. Mori, R. Scheffler, A. Speidel, M. Sherwood, A. C. Luntz, *J. Phys. Chem. Lett.* **2012**, *3*, 3043 – 3047.
[7] N. Tsiouvaras, S. Meini, I. Buchberger, H. A. Gasteiger, *J. Electrochem. Soc.* **2013**, *160*, A471 – A477.
[8] H. Beyer, S. Meini, N. Tsiouvaras, M. Piana, H. A. Gasteiger, *Phys. Chem. Chem. Phys.* **2013**, *15*, 11025 – 37.
[9] M. M. Ottakam Thotiyl, S. A. Freunberger, Z. Peng, P. G. Bruce, *J. Am. Chem. Soc.* **2013**, *135*, 494 – 500.
[10] D. G. Kwabi, N. Ortiz-Vitoriano, S. A. Freunberger, Y. Chen, N. Imanishi, P. G. Bruce, Y. Shao-Horn, *MRS Bull.* **2014**, *39*, 443 – 452.
[11] J. Hassoun, F. Croce, M. Armand, B. Scrosati, *Angew. Chem. Int. Ed.* **2011**, *50*, 2999 – 3002; *Angew. Chem.* **2011**, *123*, 3055 – 3058.
[12] Q. Li, F. Chen, W. Zhao, M. Xu, B. Fang, Y. Zhang, L. Duo, Y. Jin, F. Sang, *Bull. Korean Chem. Soc.* **2007**, *28*, 1656 – 1660.
[13] W. Adam, D. V. Kazakov, V. P. Kazakov, *Chem. Rev.* **2005**, *105*, 3371 – 3387.
[14] Y.-C. Lu, H. A. Gasteiger, M. C. Parent, V. Chiloyan, Y. Shao-Horn, *Electrochem. Solid-State Lett.* **2010**, *13*, A69 – A72.
[15] F. Wilkinson, W. P. Helman, A. B. Ross, *J. Phys. Chem. Ref. Data* **1995**, *24*, 663.
[16] M. M. Richter, *Chem. Rev.* **2004**, *104*, 3003 – 3036.
[17] P. Bruce, S. Freunberger, L. Hardwick, J.-M. Tarascon, *Nat. Mater.* **2012**, *11*, 19 – 30.
[18] M. Balaish, A. Kraytsberg, Y. Ein-Eli, *Phys. Chem. Chem. Phys.* **2014**, *16*, 2801 – 2822.
[19] R. Black, J.-H. Lee, B. Adams, C. A. Mims, L. F. Nazar, *Angew. Chem. Int. Ed.* **2013**, *52*, 392 – 396; *Angew. Chem.* **2013**, *125*, 410 – 414.
[20] J. Wandt, C. Marino, P. Jakes, R. Eichel, H. A. Gasteiger, J. Granwehr, *Energy Environ. Sci.* **2015**, *8*, 1358 – 1367.
[21] Y. Lion, M. Delmelle, A. Van de Vorst, *Nature* **1976**, *263*, 442 – 443.
[22] R. Konaka, E. Kasahara, W. C. Dunlap, Y. Yamamoto, K. C. Chien, M. Inoue, *Free Radical Biol. Med.* **1999**, *27*, 294 – 300.
[23] Z.-Z. Ou, J.-R. Chen, X.-S. Wang, B.-W. Zhang, Y. Cao, *New J. Chem.* **2002**, *26*, 1130 – 1136.
[24] I. Rosenthal, C. M. Krishna, G. C. Yang, T. Kondo, P. Riesz, *FEBS Lett.* **1987**, *222*, 75 – 78.
[25] P. R. Ogilby, *Chem. Soc. Rev.* **2010**, *39*, 3181 – 3209.
[26] C. Schweitzer, R. Schmidt, *Chem. Rev.* **2003**, *103*, 1685 – 1757.
[27] K. U. Schwenke, M. Metzger, T. Restle, M. Piana, H. A. Gasteiger, *J. Electrochem. Soc.* **2015**, *162*, A573 – A584.
[28] M. Kavala, R. Boča, L. Dlháň, V. Brezová, M. Breza, J. KožíŠek, M. Fronc, P. Herich, L. Švorc, P. Szolcsányi, *J. Org. Chem.* **2013**, *78*, 6558 – 6569.
[29] J. L. Hodgson, M. Namazian, S. E. Bottle, M. L. Coote, *J. Phys. Chem. A* **2007**, *111*, 13595 – 13605.
[30] B. J. Bergner, A. Schu, K. Peppler, A. Garsuch, J. Janek, *J. Am. Chem. Soc.* **2014**, *136*, 15054 – 15064.
[31] G. Nardi, I. Manet, S. Monti, M. A. Miranda, V. Lhiaubet-Vallet, *Free Radical Biol. Med.* **2014**, *77*, 64 – 70.

Received: March 1, 2016
Published online: April 26, 2016

